



## EXPERIMENTAL AND NUMERICAL INVESTIGATION OF THE MECHANICAL BEHAVIOUR OF AN OPEN-CELL CERAMIC FOAM UNDER MULTIAXIAL LOADINGS

O. Kraiem <sup>1\*</sup>, M. Houillon <sup>2</sup>, N. Schmitt<sup>1</sup> and H. Zhao<sup>1</sup>

<sup>1</sup>LMT-Cachan UMR 8535  
ENS Cachan, CNRS, Université Paris Saclay  
Bâtiment Léonard de Vinci  
61 avenue du Président Wilson  
94230 Cachan

Email: kraiem@lmt.ens-cachan.fr, schmitt@lmt.ens-cachan.fr, zhao@lmt.ens-cachan.fr

<sup>2</sup> TN International  
1 Rue des Hrons, 78180 Montigny-le-Bretonneux  
Email: marie.houillon@areva.com

### ABSTRACT

*In this study, an experimental and numerical investigation regarding the mechanical behavior of open-cell ceramic-like foam (OCCF) was carried out. The aim was to identify a continuum model able to predict the mechanical response under complex path loadings. Uniaxial and true triaxial tests have been done to investigate the compression behavior of OCCF. Elastic-brittle behavior is observed under uniaxial unconfined compression loading while a crushing plateau with high-energy absorption capacity is exhibited under uniaxial confined compression. Limited strain rate dependence is found. The experimental results are discussed and correlated with degradation mechanisms identified by X-ray computed tomography observation. Tested under multiaxial loadings, the OCCF exhibits slightly transversely isotropy. Also its yield surface has been well described by a Deshpande-Fleck yield criterion. The Deshpande-Fleck model for foam has been modified by introducing a dependence of the plastic Poisson's coefficient with the plastic volumetric strain to improve the prediction of the radial expansion. It has been implemented into the finite-element code LS-Dyna via a usermat subroutine. Numerical results are in close agreement with the experimental results.*

## 1 INTRODUCTION

In recent years, Open-Cell Ceramic-like Foams (OCCF) are widely used in many industrial applications thanks to their physical and thermo-mechanical properties such as low density, low thermal conductivity, high compressive strength to weight ratio and high fire resistance [1],[2],[3]. Due to its ability to accommodate large deformation, OCCF is a promising candidate for energy absorption engineering applications, provided that foam parts are encapsulated by a ductile housing to avoid mass loss during the crushing. In that case foams can be subjected to complex multiaxial stress states. Consequently, performing simple uniaxial compression tests without or with lateral confinement at different strain rates is not sufficient to identify a mechanical model. It is therefore necessary to characterize the behavior under multiaxial loadings.

The mechanical characterization of brittle foams under complex loadings is scarcely found in the literature unlike that of ductile foams. To understand the compressive behavior and estimate the failure envelope of polymeric and metallic foams, Deshpande et al. [4],[5] have developed two high-pressure triaxial systems allowing to apply a particular multiaxial loading paths on cylindrical and cubic samples. Canto [6], developed a true triaxial compaction device composed of six sliding blocks to study the triaxial behavior of very compressible materials and powders allowing to explore more complex triaxial loading paths and for very large strains [7][8].

In this research, the mechanical response of low density OCCF has been characterized at room temperature under uniaxial and multiaxial loadings and notably its yield surface has been identified. Thanks to X Rays Computer Tomography observation on samples subjected to oedometric compression test stopped a different load, the mechanisms of degradation has also been identified and correlated to the change in behavior noted on the Force - displacement curves. An extension of Deshpande Fleck criterion[4] is proposed to predict the OCCF experimental data. The identified model has been implemented as a user-defined material model in the finite element code LS-DYNA[9], and numerical simulations of crushing tests were carried out in order to validate this model.

## 2 EXPERIMENTAL CHARACTERIZATION

### 2.1 Material : microstructure, specimens geometry and procedures

The OCCF foams used in this experimental study was manufactured by direct carbonization of a polymeric foam. The apparent bulk density of the OCCF material is about  $\rho_a = 250 \text{ kg.m}^{-3}$  and its porosity is equal to  $n = 82 \%$ . A typical microstructure is shown in Fig. 1. Like most foams, it is characterized by cells, empty pores and ligaments connecting cells together. The characteristic cell-size ranges from  $50 \mu\text{m}$  to  $150 \mu\text{m}$ . Small-pores, the size of which being lower than  $10 \mu\text{m}$ , are also observed on the wall of the cells. Due to the manufacturing process, the microstructure of this material is slightly elongated in the foaming direction (Fig 1b) and explains the slightly anisotropy observed during the tests.

Quasi-static compression tests with and without lateral confinement were conducted on cubical ( $a = 40 \text{ mm}$ ) and cylindrical specimens ( $D = 30 \text{ mm}$ ,  $H = 30 \text{ mm}$ ) by using an Universal hydraulic testing machine Instron. A Split Hopkinson Pressure Bar (SHPB) system was used to study the strain rate sensitivity of the OCCF foams. Cylindrical samples ( $D = 22 \text{ mm}$ ,  $H = 9 \text{ mm}$ ) were used for that analysis. Ex-situ quasi-static compression tests with X-ray computed tomography analysis were performed on cylinders ( $D = 30 \text{ mm}$ ,  $H = 30 \text{ mm}$ ) to investigate their failure mechanisms. Triaxial tests were conducted on cubes to study the multiaxial behavior by using Cantos compaction device (Fig. 2a) installed in the triaxial testing

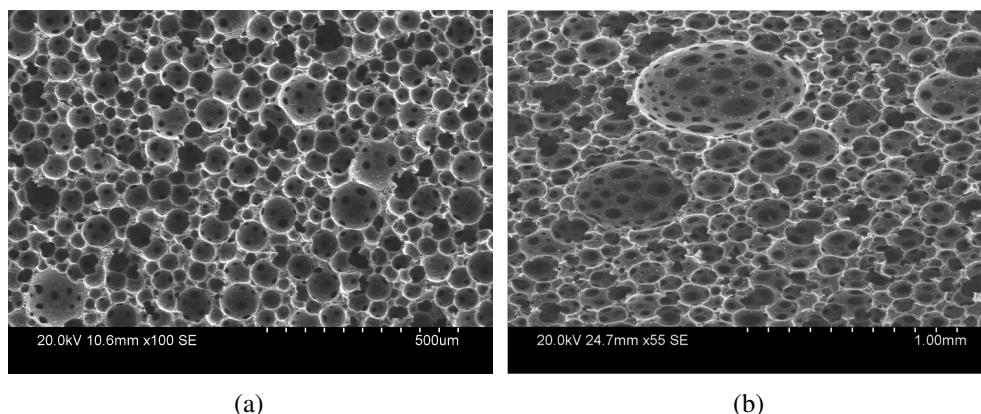


Figure 1. SEM micrographs of the OCCF foam

machine ASTREE. ASTREE comprises six independent actuators paired up along the three perpendicular directions pushing the blocks to reduce the hole, each one sliding relative to the others. During the triaxial tests, the imposed displacements on the cubical specimen in each direction were measured by laser displacement sensors (Fig. 2b).

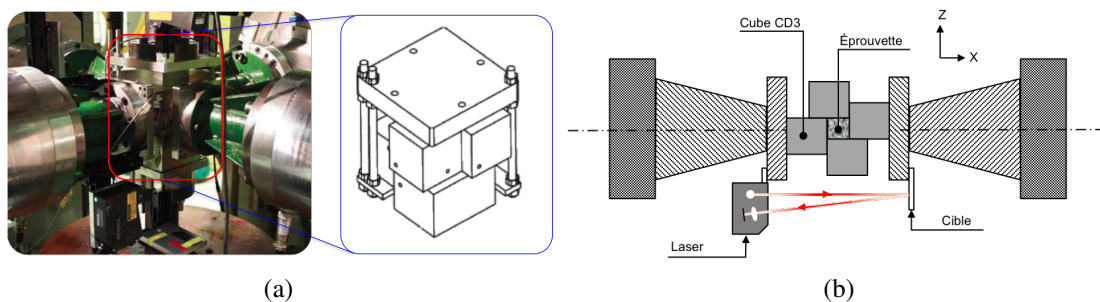


Figure 2: Triaxial compression test: a) compaction device installed in the ASTREE testing machine b) Actuators displacement measurement with a laser sensor

## 2.2 Experimental results

Typical compressive stress-strain curves of an OCCF subjected to quasi-static loading ( $V = 5 \text{ mm} \times \text{min}^{-1}$ ) with and without lateral confinement, is shown in Fig. 3. The stress-strain curve obtained during unconfined compression test reveals the elastic-brittle behavior of that the foam has an elastic-brittle behaviour (Fig. 3a). When lateral displacement is prevented under confined conditions the compression behavior is significantly different (Fig. 3b). Three zones can be highlighted: first a short elastic range with a brittle failure, then a crushing plateau and finally a densification with an increase in stiffness and stress. Fig. 3c shows the slightly anisotropic compressive response when the OCCF specimens are loaded in three directions (i.e., for angles 0, 45 and 90). The dynamic stress-strain curves of OCCF under confined conditions are shown in Fig. 3d. Comparing the dynamic compressive and confined behavior to those obtained under quasi-static conditions permits to show the responses are close to each other (elastic regime, plateau and densification) and confirms a low sensibility of the mechanical behavior to the applied strain rate compared with other cellular materials the compressive properties look good for structural applications, notably its ability to absorb a large amount of energy under impact loadings.

To understand the damage mode and the crush mechanisms of the brittle ceramic foams under impact, an ex-situ compression test was performed on a confined cylindrical sample. The test

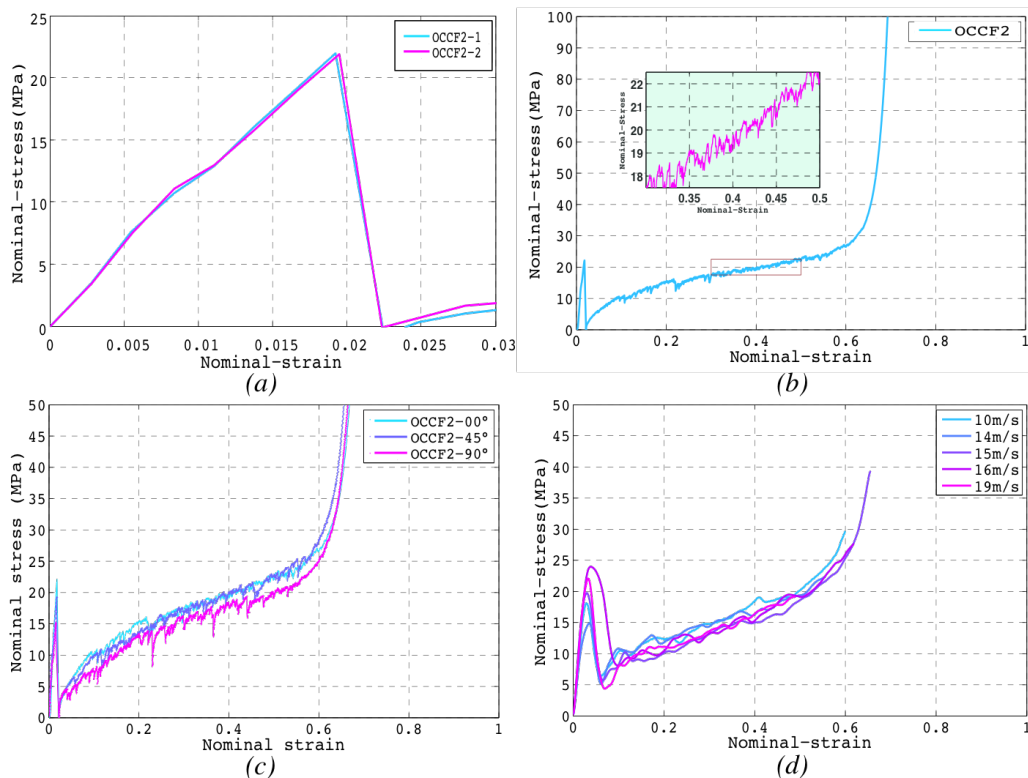


Figure 3: Uniaxial compression stress-strain curves: a) static compression behavior without confinement, b) static compression behavior with lateral confinement, c) Static anisotropic compression behavior with lateral confinement in three loading directions and d) dynamic compression behavior

was interrupted at different strain levels and scans were taken with a X-rays CT tomograph at each step. Analysis of the 3D images has enable tracking the mechanisms of deformation during the test. They have shown that the non linear deformation of the OCCF are controlled by the appearance of crushing bands in the sample which lead to the fragmentation of foam into parts becoming more and more smaller until it has been transformed into powder at the end of the densification. Figure 4 shows the force-displacement curve registered during the ex-situ compression test and cross-sectional tomography images at each step.

Triaxial compression tests were performed with a triaxial testing machine "ASTREE" to characterize the OCCF multiaxial behavior. Iso-displacement compaction pression loading, oedometric compression loading and more complex triaxial compression loading with variable confining pressure were carried out under quasi-static conditions ( $5 \text{ mm} \times \text{min}^{-1}$ ). In these tests, the samples inside the compacting device have been oriented along in such way that their foaming direction was parallel to the vertical axis of the ASTREE machine *axis 3*. Under iso-displacement compression loading (i.e., same compression loading rate applied along the three perpendicular directions), the material exhibits a slightly transversely isotropic behavior (stress-volumetric strain curves drawn on Fig. 5a). The compressive strength in the rise foaming direction *axis 3* is higher than that in perpendicular directions (*axis 1* and *axis 2* directions). In another triaxial test the foam sample was compressed by applying the same displacement rate in the three directions until the first brittle failure was reached and then it was loaded axially (uniform compression force rate in direction *axis 3*) while keeping constant the confining pressure in the perpendicular directions *axis 1* and *axis 2*. These experiments exhibit clearly the influence of the lateral confinement on the mechanical response of OCCF. Figure 5b shows the variation of the curves stress-volumetric strain when varying lateral confinement from 5KN to 25KN.

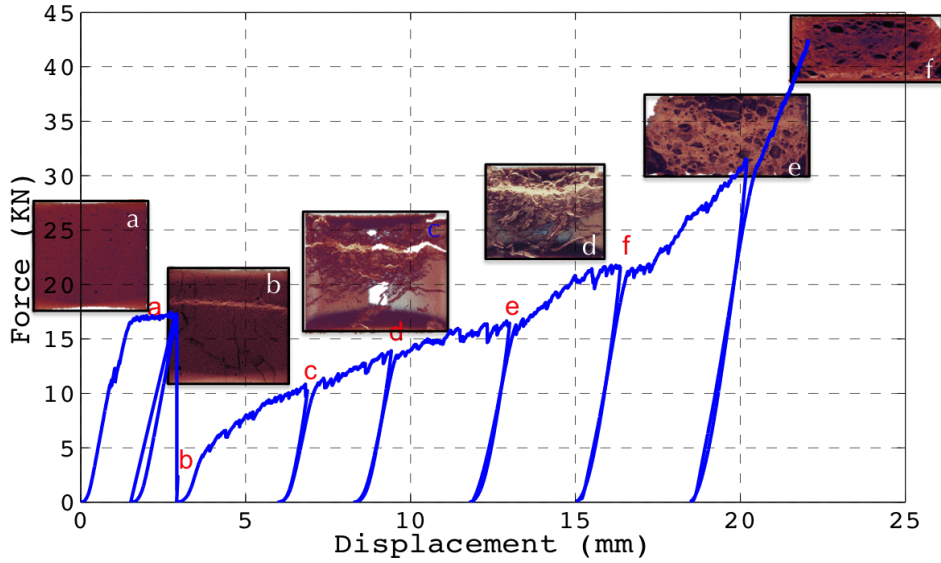


Figure 4: Force versus displacement curve and microstructural change obtained by tomographic analysis of the OCCF from the ex-situ confined compression test

Experimental data have been used to identify the yield surface of the brittle ceramic foam. The

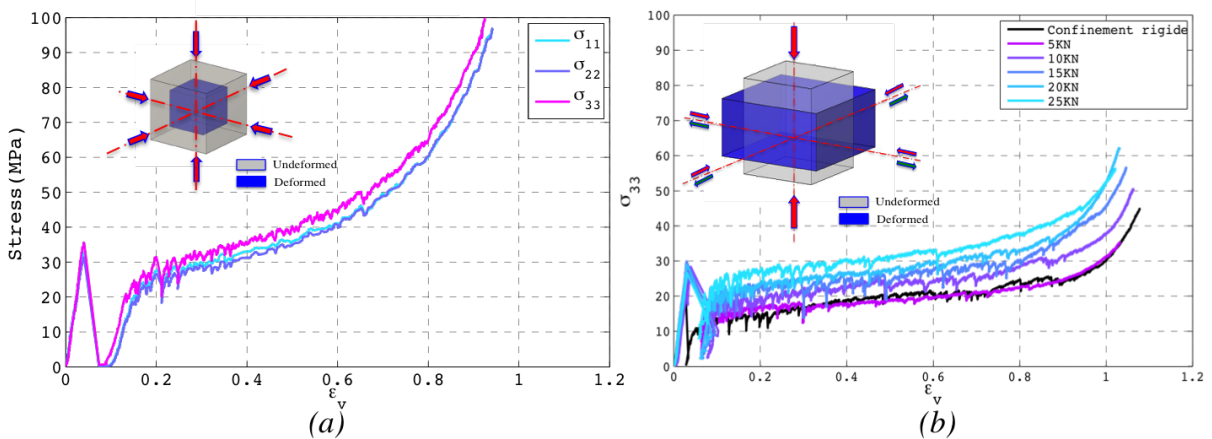


Figure 5: Triaxial compression tests on OCCF samples: a) response of the material under a hydrostatic loading, b) Effect of the lateral confining pressure on the response of the material

failure surfaces and its evolution were constructed in mean stress ( $\sigma_m = -\frac{1}{3}(\text{tr}\boldsymbol{\sigma})$ ) versus deviatoric stress ( $\sigma_d = \sqrt{\frac{3}{2}\boldsymbol{s} : \boldsymbol{s}}$ ) space for various levels of volumetric strain. The obtained behavior seems to be adjusted by an elliptic yield criterion in the compressive zone of the space  $\sigma_m - \sigma_d$  defined by :

$$\Phi = \hat{\sigma}^2 - Y^2 = \frac{1}{[1 + (\frac{\alpha}{3})^2]} [\sigma_e^2 + \alpha^2 \sigma_m^2] - Y^2 \quad (1)$$

This relationship corresponds to the Deshpande Fleck criterion. To account for a good description of the hardening of the material during the densification, the initial Deshpande & Fleck model has been improved to predict the radial anelastic expansion in the plastic domain (called MDF model). Where  $\sigma_e$  is the von Mises effective stress and  $\sigma_m$  is the hydrostatic stress. The parameter  $\alpha$  defines the shape of the yield surface given by

$$\alpha = \frac{9}{2} \frac{1 - 2\nu^p}{1 + \nu^p} \quad (2)$$

where  $\nu^p$  is the plastic coefficient defined as a function of the plastic volumetric strain.

Figure 6.b shows the evolution of the OCCF yield surfaces fitted by the Modified Deshpande & Fleck (MDF) yield surface.

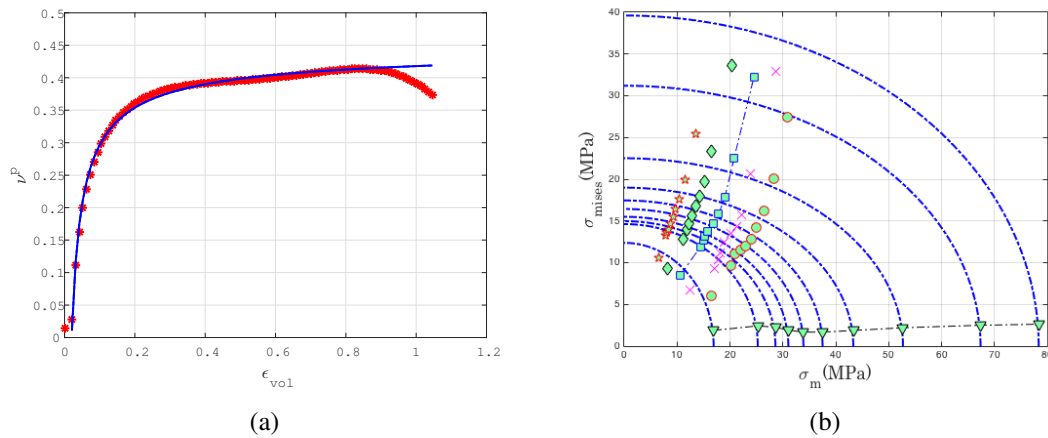


Figure 6: Identification of the MDF parameters model for the OCCF: a) variation of the plastic Poisson's Ratio b) Yield surface in mean stress-deviatoric stress space

### 3 NUMERICAL SIMULATION

The MDF model has been implemented via an usermat subroutine in the finite element code LS-DYNA. In order to validate the behavior model and to verify its applicability to simulate crushing tests in quasistatic conditions. The crushing test consists to apply an inclined ( $15^\circ$ ) on a cylindrical OCCF part enclosed in a metallic jacket where behavior is described by the piecewise-linear-plasticity material model. Fig.7a shows the deformation map obtained at the last step of the loading. For each test the overall force  $\rho$  overall displacement curve was recorded. A comparison of the force versus displacement curves from testing and simulation are shown in Fig.7b. Comparison between the simulation model from the inclined test showed that the MDF model gives a realistic description of the test.

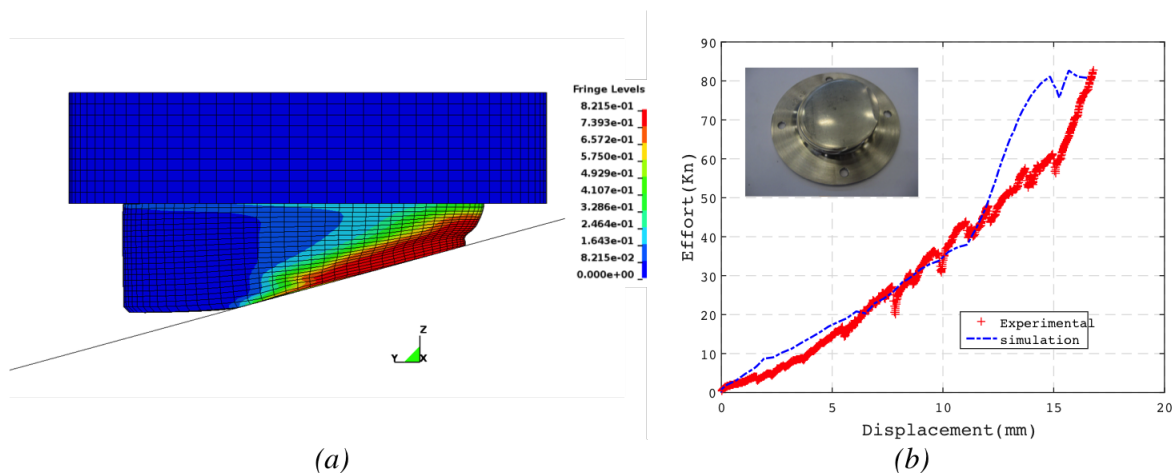


Figure 7: Finite element simulation of crushing test: a) residual deformation of the structure at the end of loading and equivalent plastic strain distribution on the OCCF part. b) comparison of experimental and numerical force-displacement curves from inclined crushing test.

## 4 CONCLUSIONS

In this work a exhaustive characterization of the brittle ceramic foam (OCCF) has been presented. A slightly modified Deshpande and Fleck model is identified in which both the slightly transversely isotropy due to the manufacturing process and slightly time dependence are not taken into account in this first model. First analysis of the experimental data permitted to identify an elliptic yield criterion depending on the level of volumetric plastic strain. The constitutive equations have been implemented into LS-Dyna FE code. First numerical results shows a good agreement compared to the experimental results. Further investigation is required to model the transversely isotropically behavior of the OCCF foam and the strong tension-compression assymetry that is observed for this material.

## REFERENCES

- [1] Paolo Colombo Michael Scheffler. *Cellular Ceramics: Structure, Manufacturing, Properties & Applications*. Weinheim: Wiley-VCH, 2005.
- [2] J.M. Gmez de Salazar, M.I. Barrena, G. Morales, L. Matesanz, and N. Merino. Compression strength and wear resistance of ceramic foams-polymer composites. *Materials Letters*, 60(13-14):1687 – 1692, 2006.
- [3] M.Houillon. Shock-absorbing protection element for packaging for the transport and/or temporary storage of radioactive materials, 2015.
- [4] V.S. Deshpande and N.A. Fleck. Isotropic constitutive models for metallic foams. *Journal of the Mechanics and Physics of Solids*, 48(67):1253 – 1283, 2000.
- [5] V.S Deshpande and N.A Fleck. Multi-axial yield behaviour of polymer foams. *Acta Materialia*, 49(10):1859 – 1866, 2001.
- [6] Rodrigo Bresciani Canto. *Theoretical and experimental study of the compaction and sintering processes of polytetrafluoroethylene (PTFE)*. Theses, École normale supérieure de Cachan - ENS Cachan, August 2007.
- [7] Carole Frdy, Rodrigo B. Canto, Nicolas Schmitt, Stphane Roux, and Ren Billardon. Modelling of the mechanical behaviour of two pure ptfe powders during their compaction at room temperature. *AIP Conference Proceedings*, 1542(1), 2013.
- [8] Omar Kraiem, Nicolas Schmitt, and Han Zhao. Experimental investigation of mechanical behaviour of brittle foam under multiaxial loading. ICEM16, 2014.
- [9] J.O.Hallquist. *Ls-dyna theoretical manual*. May 1998.

## COPYRIGHT NOTICE

Copyright ©2015 by the authors. Distribution of all material contained in this paper is permitted under the terms of the Creative Commons license Attribution-NonCommercial-NoDerivatives 4.0 International (CC-by-nc-nd 4.0).

